

PAPER

Reinterpreting the energy dependence of the optical potential

To cite this article: L C Chamon and L R Gasques 2016 *J. Phys. G: Nucl. Part. Phys.* **43** 015107

View the [article online](#) for updates and enhancements.

You may also like

- [Improved multi-position calibration for inertial measurement units](#)
Hongliang Zhang, Yuanxin Wu, Wenqi Wu et al.
- [Entanglement of 1s0d-shell nucleon pairs](#)
E Kwaniewicz
- [Subthreshold and near-threshold kaon and antikaon production in proton–nucleus reactions](#)
A V Akindinov, M M Chumakov, M M Firoozabadi et al.

Reinterpreting the energy dependence of the optical potential

L C Chamon¹ and L R Gasques^{1,2}

¹ Departamento de Física Nuclear, Instituto de Física da Universidade de São Paulo, Caixa Postal 66318, 05315-970, São Paulo, SP, Brazil

² INFN, Sezione di Napoli, Naples, Italy and Dipartimento di Matematica e Fisica Seconda Università degli studi di Napoli, Caserta, Italy

E-mail: lchamon@if.usp.br

Received 23 June 2015, revised 3 August 2015

Accepted for publication 18 September 2015

Published 10 December 2015



CrossMark

Abstract

In earlier works, we proposed a model for the nuclear potential of α -nucleus systems which is energy independent and has no adjustable parameters. This interaction has been successfully applied in the description of fusion, elastic and inelastic scattering data for many of those systems in regions of low energy. In the present work, we assume the same interaction as the bare potential to study the elastic scattering for $\alpha + {}^{208}\text{Pb}$ in a wide energy range. We demonstrate that the corresponding data set can be described if couplings to inelastic states with high excitation energy are explicitly considered through coupled-channel calculations.

Keywords: coupled-channel formalism, optical model, optical potential

(Some figures may appear in colour only in the online journal)

1. Introduction

The collision between two nuclei can result in several processes, such as elastic and inelastic scattering, transfer reactions, fusion, break-up, etc. Due to the many nucleons involved, the corresponding large number of degrees of freedom makes the theoretical description of these processes very challenging. The couplings among the different reaction channels can significantly affect the respective cross sections obtained in theoretical calculations. For instance, the couplings to inelastic and transfer channels can result in an enhancement of several orders of magnitude for the fusion cross sections at sub-Coulomb energies (see e.g. [1, 2]). Thus, the coupled-channel (CC) formalism has been often assumed in data analyses. However, due to limitations related to the numerical calculations, the number of states explicitly considered in

the coupled equations is in general not very large, mostly low-lying inelastic and transfer states.

Elastic scattering is the simplest process that occurs in a nuclear collision since it involves the least amount of matter and energy rearrangement. A huge amount of experimental data for this process has been obtained for many systems and energies. The optical model has been assumed in many works that deal with elastic scattering data analyses. In this approach, the theoretical calculations are performed assuming a simple one-channel Schrödinger equation with a complex optical potential (OP). In this context, an important energy-dependence of the phenomenological OP has been reported (see e.g. [3]). Several theoretical models have been developed to account for this energy dependence, such as, for instance, the variety of density- and energy-dependent interactions (e.g. [4, 5]), the parameter-free São Paulo potential [6] and the Lax interaction (e.g. [7]). In most of these models, the real part of the OP is obtained from double-folding procedures and the energy dependence is associated to the effective nucleon-nucleon interaction. The imaginary part can also be derived in a similar form, in the context of the Lax interaction, or most often be assumed within a phenomenological approach, that includes the use of simple shapes such as in Woods-Saxon shape.

In earlier works [8–10], we proposed a theoretical model for the nuclear potential of α -nucleus systems, which is energy independent and has no adjustable parameters. This interaction has been successfully applied in the description of fusion, elastic and inelastic scattering data for many systems at low energy regions [8–10]. In the present work, we assume the same interaction as the bare potential to study the elastic scattering for $\alpha + {}^{208}\text{Pb}$ in a wide energy range. We demonstrate that the corresponding data set can be described if couplings to inelastic states with high excitation energies are explicitly considered through CC calculations. Since the bare interaction is energy independent, our results indicate that the observed energy dependence of the phenomenological OP can be associated to the effect of these couplings.

2. Theoretical framework

According to [8–10], we assume for the real part of the bare nuclear potential the following:

$$V_N(R) = \int \rho_1(r_1) \rho_2(r_2) v(\vec{R} - \vec{r}_1 + \vec{r}_2) d\vec{r}_1 d\vec{r}_2, \quad (1)$$

with

$$v(\vec{r}) = -U_0 e^{-(r/a)^2}, \quad (2)$$

where $U_0 = 87.226 \text{ MeV}$, $a = 0.95 \text{ fm}$, and the $\rho_i(r_i)$ represent the matter densities of the nuclei. For the α particle, we assume that the matter density has the same shape of the corresponding ${}^4\text{He}$ charge distribution (from [11]). We adopt the systematics of the matter distributions of the São Paulo potential [6] for the ${}^{208}\text{Pb}$.

The imaginary part of the OP assumed in our calculations has the Woods–Saxon shape:

$$W(R) = -\frac{W_0}{1 + \exp[(R - R_{I0})/a_I]}, \quad (3)$$

with $R_{I0} = r_{I0}(A_1^{1/3} + A_2^{1/3})$. The values of the corresponding parameters were carefully studied and obtained in [10], assuming that the absorption of flux by the imaginary part of the OP should only simulate the fusion process without affecting the barrier tunneling: $W_0 = 60 \text{ MeV}$, $r_{I0} = 0.8 \text{ fm}$ and $a_I = 0.25 \text{ fm}$.

In [10], this OP (real and imaginary parts) was assumed in the fusion, elastic and inelastic scattering data analyses for many α -nucleus systems. In that work, CC calculations were performed to obtain the corresponding cross sections, in which a small number of low-lying inelastic states (first 2^+ and 3^- states of even–even target nuclei) were explicitly considered in the coupled equations. The analyses only involved data at energies around the Coulomb barrier and the following results were obtained:

- (1) the experimental fusion cross sections were very well reproduced by the theoretical calculations in the complete energy region;
- (2) the elastic and inelastic data were very well reproduced at sub-Coulomb energies;
- (3) at energies above the barrier, the elastic experimental cross sections were well reproduced at forward angles ($\theta \leq \theta_{1/4}$, where $\theta_{1/4}$ represents the quarter-point angle), but the theoretical results largely underestimate the cross sections at the backward angular region;
- (4) similar behavior was observed for the inelastic scattering cross sections at energies above the barrier;
- (5) the couplings to the low-lying inelastic states do not significantly affect the theoretical elastic scattering cross sections.

In order to understand these results, a few simulations were performed in that work. These simulations indicated that, for the above-barrier energies, the couplings to inelastic states of high excitation energies could provide quite important contributions to the elastic scattering cross sections at backward angles. Indeed, this conclusion has motivated the present work.

We have chosen $\alpha + {}^{208}\text{Pb}$ to be studied because there are many experimental sets of elastic scattering angular distributions for this system in a very wide energy range. Furthermore, also inelastic processes have been measured at low and high energies. In particular, the data sets reported in [12, 13] are important for the present work, because they provide the inelastic cross sections of states with high excitation energy. Data for $\alpha + {}^{208}\text{Pb}$ at $E_{\text{LAB}} = 120$ MeV were obtained in those works. Besides the presence of some particular states observed with excitation energies up to about 10 MeV, the corresponding spectra show a quite large background beyond the giant resonance region, which reaches excitation energies up to about 50 MeV (see e.g. figure 1 of [12]). This continuum background is due to real nuclear scattering processes and is, of course, observed in all reaction studies on giant resonances. The nature of this background has been studied in [13]. In those measurements, the spectra were taken at and around 0 degrees. In that experiment, special care was taken to remove the instrumental background due to beam halos and slit scattering. Furthermore, by studying neutron decay at forward and backward angles, it was possible to separate the nuclear continuum into its two components: the neutron knock-out contribution correlated with neutrons emitted at forward angles and the contribution due to single and multiple inelastic excitations of ${}^{208}\text{Pb}$ states with neutrons emitted more or less isotropically.

In order to estimate the cross section related to the inelastic processes in the case of $\alpha + {}^{208}\text{Pb}$ at $E_{\text{LAB}} = 120$ MeV, we have adjusted the corresponding angular distributions provided in figure 8 of [12], within the DWBA formalism, with OP and deformation parameters adjusted to fit the data. We obtained a total (integrated in angle and excitation energy) cross section of about 24 mb for states with excitation energy up to about 7 MeV. By assuming that the total cross section is proportional to the counts obtained in the spectrum of figure 1 of [12], we estimated a cross section of about 200 mb in the region of excitation energy of $2.6 \leq E^* \leq 50$ MeV. Probably, there is more contribution from states with $E^* > 50$ MeV. Thus, at $E_{\text{LAB}} = 120$ MeV, the inelastic processes can be associated to cross sections of the order of magnitude of hundreds of millibarns.

The most adequate method for solving a problem involving a large number of nucleons would be to perform CC calculations including all inelastic states up to very high excitation energies. However, due to the huge number of states, there are prohibitive limitations in the corresponding computational numerical calculations. Systematics for the density of nuclear levels has been performed in [14], where it is parametrized as:

$$\rho(E^*) = \frac{1}{T} e^{(E^* - E_0)/T}. \quad (4)$$

In the case of ^{208}Pb , the suggested parameters values are: $T = 1.06$ MeV and $E_0 = 0.52$ MeV. The semi-closed symbols in figure 1 represent the number of nuclear levels as a function of the excitation energy, for ^{208}Pb , obtained with (4). N is the number of levels in the interval of ± 0.5 MeV around E^* . For the purpose of comparison, the closed symbols in the figure represent the number of levels obtained in the data basis of the National Nuclear Data Center (NNDC). Expression (4) results in a total of about 10^{20} levels in the region $E^* \leq 50$ MeV. Of course, usual CC calculations involving so many states are totally impracticable.

In order to study the effects of couplings to inelastic states with high E^* on the elastic cross sections, we have coupled only a few states, within the framework of the rotational model, using relatively large deformation parameters with the purpose of simulating the effect of myriad of states. The deformation was applied only in the real part of the nuclear interaction and the calculations were performed with the FRESCO code [15]. The spin and excitation energies related to these couplings are presented in table 1. The adopted deformation parameters are $\delta_2 = 3.5$ fm and $\delta_3 = 3.0$ fm, which are much larger than the values assumed in [10] for the 2^+ and 3^- low-lying ^{208}Pb states: $\delta_2 = 0.40$ fm and $\delta_3 = 0.78$ fm. Note that the 2^+ and 3^- states are coupled in first order through δ_2 and δ_3 , respectively, while the 4^+ states are coupled in second order through δ_2 .

3. Data analyses

We have obtained experimental elastic scattering angular distributions for $\alpha + ^{208}\text{Pb}$ from [16–21] (part of these data were taken from the EXFOR data basis). The corresponding bombarding energy range is from $E_{\text{LAB}} = 20$ MeV to 340 MeV. The highest energy (85 MeV/nucleon) corresponds to a velocity of about 40% of the speed of light. Even so, we believe that possible corrections in our results for this case due to relativity are not much significant since $v^2/c^2 \approx 0.16$.

The parameter values of the couplings adopted in our CC calculations have been obtained from qualitative adjustments of the corresponding cross sections with the data for 340 MeV. Unfortunately, we could not include more states, with higher excitation energies, since the corresponding CC calculations do not converge. Having the parameter values fixed, we extrapolated the calculations to lower energies. The number of coupled states for each bombarding energy was determined in such form that the numerical convergence of the CC calculations was achieved. Thus, we did not coupled states with the highest excitation energies for the angular distributions taken at 58, 104 and 139 MeV. Table 2 provides the maximum number of states coupled for each angular distribution. The table also provides the total inelastic and fusion cross sections obtained with and without couplings. For above-barrier energies, the couplings enhance the fusion by less than 7%, while for the below-barrier energy ($E_{\text{LAB}} = 20$ MeV) the corresponding enhancement is 25%.

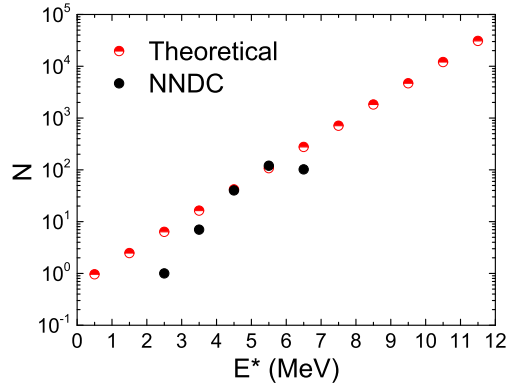


Figure 1. The number of nuclear levels as a function of the excitation energy for ^{208}Pb . N represents the number of levels in intervals of ± 0.5 MeV around E^* . The semi-closed symbols represent the results of (4) while the closed symbols are experimental results obtained from the National Nuclear Data Center (NNDC).

Table 1. Values of the excitation energies (MeV) and spin of the couplings adopted in our CC calculations.

State	E^*	spin
1	5	2^+
2	20	3^-
3	30	4^+
4	37	4^+
5	50	4^+
6	60	4^+

Table 2. The table provides, for each angular distribution, the maximum number of coupled states (N), the total inelastic cross section (σ_{In} —mb), the fusion cross section (mb) obtained from the CC calculation (σ_{CC}) or without couplings (σ_{WC}).

E_{LAB} (MeV)	N	σ_{In}	σ_{CC}	σ_{WC}
20	6	0.0095	55.5	44.2
23.6	6	2.44	445	430
27.6	6	18.9	878	872
58	5	88.4	2102	2054
104	4	201	2391	2301
120	4	247	2395	2308
139	4	283	2393	2257
340	6	814	1817	1711

As indicated in table 2, we have performed CC calculations at $E_{LAB} = 120$ MeV using the four first excited states of table 1. With these couplings, we have obtained a total inelastic cross section of 247 mb, which is comparable to the aforementioned experimental value of about 200 mb for $E^* \leq 50$ MeV estimated from the results of [12]. This compatibility is an indication that the small set of states of table 1 can be considered as a reasonably realistic

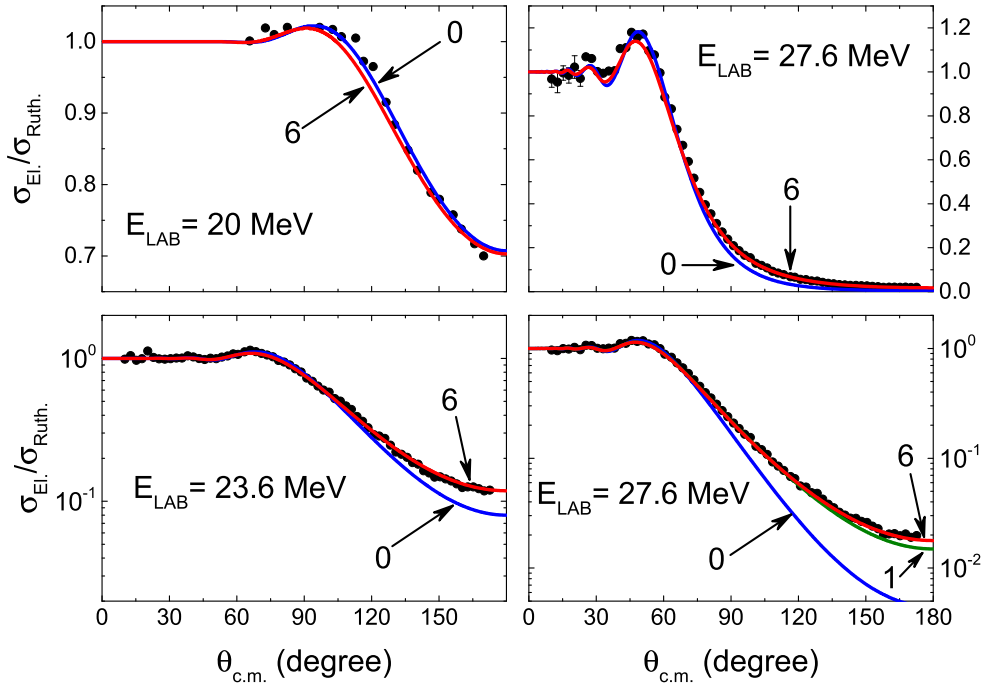


Figure 2. Elastic scattering angular distributions for $\alpha + {}^{208}\text{Pb}$ at $E_{\text{LAB}} = 20, 23.6$ and 27.6 MeV (from [16, 17]). Note the change from linear (top) to logarithmic (bottom) scales. The lines in the figure represent the CC results considering different numbers of coupled states: 0 \rightarrow no couplings; 1 \rightarrow only the first state of table 1; 6 \rightarrow all the six states of table 1.

simulation of couplings to a very large number of inelastic states with high excitation energies.

The s-wave barrier height for $\alpha + {}^{208}\text{Pb}$ corresponds, at the laboratory frame of reference, to about 20.9 MeV. Figure 2 shows three experimental elastic scattering angular distributions for energies around the barrier. The lines in the figure represent the results of the CC calculations, obtained considering different numbers of coupled states: 0 \rightarrow no couplings; 1 \rightarrow coupling only the first state of table 1; 6 \rightarrow coupling all the six states of the table. For $E_{\text{LAB}} = 20$ MeV (below barrier) the couplings almost do not affect the cross sections. At $E_{\text{LAB}} = 23.6$ MeV, the theoretical cross sections obtained coupling only the first state are almost indistinguishable from those obtained with all the six states. At backward angles, the CC cross sections are slightly larger than the results without couplings and agree very well with the data set. The angular distribution at $E_{\text{LAB}} = 27.6$ MeV was studied in detail in [10]. The theoretical cross sections obtained without couplings reproduce the data in the region $\theta \leq \theta_{1/4}$ and are in disagreement with the experimental values at the backward angular region. In [10] we showed that, adopting realistic values for the deformation parameters $\delta_2 = 0.40$ fm and $\delta_3 = 0.78$ fm, the couplings to the low-lying 2^+ ($E^* \approx 4.1$ MeV) and 3^- ($E^* \approx 2.6$ MeV) ${}^{208}\text{Pb}$ states almost do not affect the elastic cross sections. For this reason, these states were not included in the present CC calculations. On the other hand, as illustrated in figure 2, the coupling to the first state of table 1 is significant and provides CC cross sections in good agreement with the data. The couplings to the other states of table 1 are less significant and just slightly improve the agreement. The deformation of the first state of

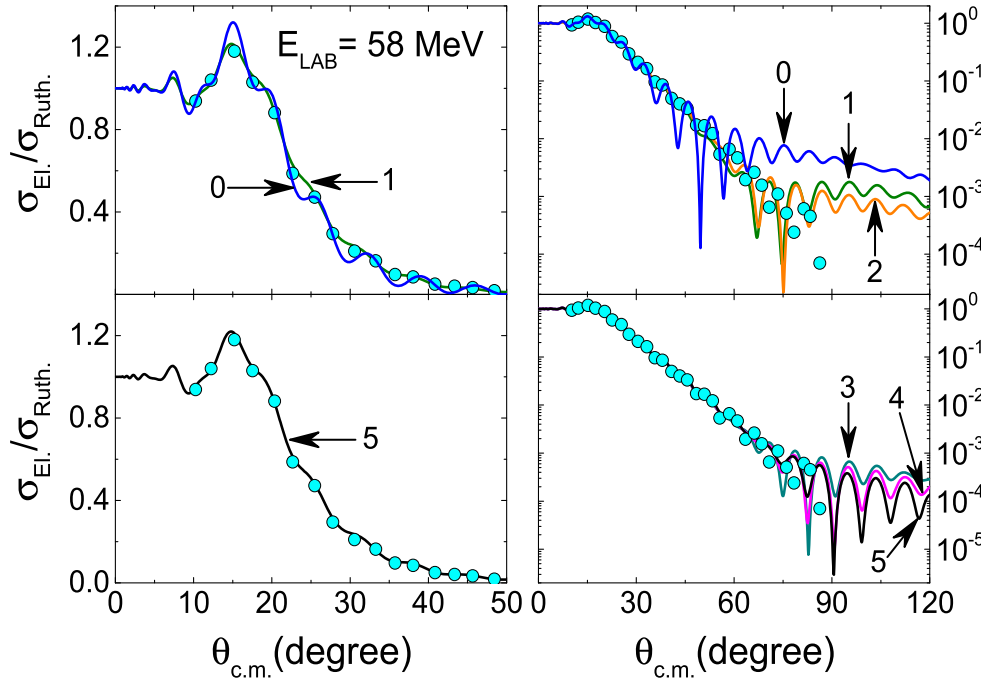


Figure 3. Elastic scattering angular distribution for $\alpha + {}^{208}\text{Pb}$ at $E_{\text{LAB}} = 58$ MeV [18]. Note the change from linear (left) to logarithmic (right) cross section scales. The lines in the figure represent the CC results considering different numbers of coupled states.

table 1, $\delta_2 = 3.5$ fm, is much larger than those for the low-lying 2^+ and 3^- states assumed in [10]. According to the present work, this state of table 1 is, in fact, simulating hundreds of states with excitation energies around 5 MeV (see figure 1).

Figure 3 presents data and theoretical results for $E_{\text{LAB}} = 58$ MeV, in linear (left) and logarithmic (right) scales. The elastic cross section plotted in the linear scale clearly shows the improvement of the agreement between data and theoretical results from the calculations without couplings (indicated by 0 \rightarrow in the figure) to those coupling the first state of table 1 (\leftarrow 1). On the other hand, the same plot in logarithmic scale reveals that the cross sections at the backward region are affected by the number of coupled states, and the results obtained with the first five coupled states of table 1 describe quite well the complete data set.

We present results for $E_{\text{LAB}} = 104$ MeV in figure 1 (top—logarithmic and bottom—linear cross section scales). It is quite illustrative the form in which the agreement between data and theoretical results significantly improves as the number of coupled states increases. Unfortunately, the numerical CC calculations with more than 4 coupled states did not converge.

The case of $E_{\text{LAB}} = 139$ MeV is shown in figure 5. The data set clearly presents a rainbow at $\theta_{\text{c.m.}} \approx 60^\circ$. Due to the computational limitation of our CC calculation, we could not couple more than the four first states of table 1. Even so, it is possible to observe in the figure that these couplings already seems to provoke the formation of a rainbow pattern.

Finally, figure 6 presents the results for $E_{\text{LAB}} = 340$ MeV. Clearly, the agreement between data and theoretical results becomes more satisfactory as the number of states included in the CC calculations increases. Probably, a much better agreement between data

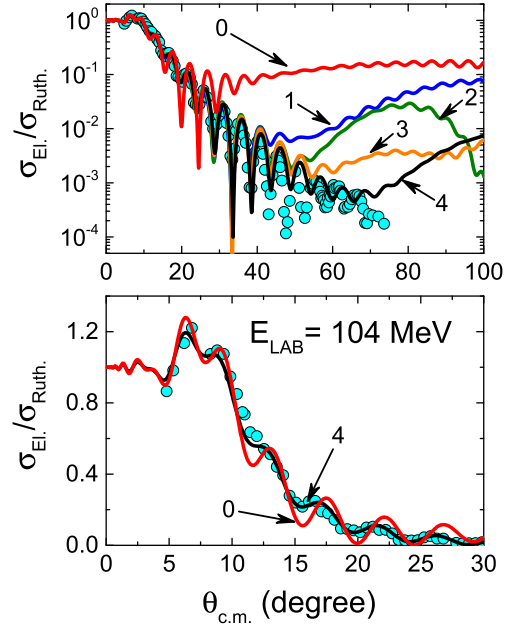


Figure 4. Elastic scattering angular distribution for $E_{\text{LAB}} = 104$ MeV [19]. Note the change from logarithmic (top) to linear (bottom) cross section scales. The lines in the figure represent the CC results considering different numbers of coupled states.

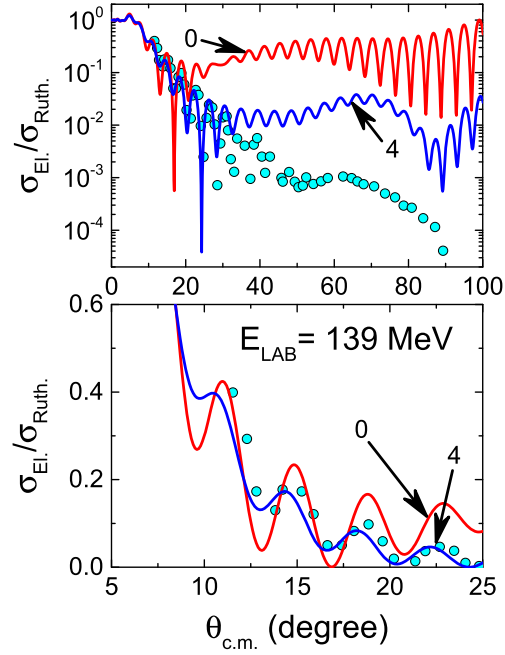


Figure 5. The same as figure 1, for $E_{\text{LAB}} = 139$ MeV [20].

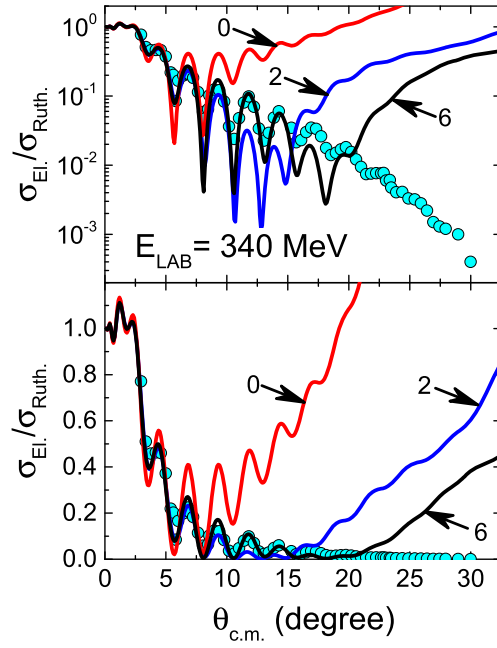


Figure 6. The same as figure 1, for $E_{\text{LAB}} = 340$ MeV [21].

and theoretical cross sections would be obtained considering many more couplings to states with excitation energies even larger than 60 MeV. However, these states with very high E^* result in numerical problems concerning the solution of the coupled equations.

4. Conclusion

CC calculations involving a large number of inelastic couplings have already been performed in other works, but generally within limited ranges of excitation and bombarding energies. For instance, about 70 states were coupled in [22] to study the fusion and quasi-elastic processes for $^{16}\text{O} + ^{208}\text{Pb}$. However, in that work the maximum excitation energy of this set of states is about 7 MeV, and the calculations were performed only for bombarding energies around the Coulomb barrier. The effect of couplings on the behavior of the OP has also been studied in several works (see e.g. [23]), but again within the limitations mentioned above. In the present work, we deal with much larger excitation energies (see table 2), and we study the effects of these couplings not only at energies around the barrier but also at intermediate energies, up to 85 MeV/nucleon. To our knowledge, this is the first time that such kind of calculations are reported.

As already commented, the bare interaction (real and imaginary parts of the nuclear potential) assumed in the present work for $\alpha + ^{208}\text{Pb}$ has provided a quite good description of the fusion, elastic and inelastic scattering processes at sub-barrier energies for many α -nucleus systems [8–10]. In the CC calculations performed in the present work, we adopted the values of the coupling parameters within a rather schematic and arbitrary form, with the purpose of simulating myriad of states with high excitation energies. The corresponding theoretical result for the total inelastic cross section at $E_{\text{LAB}} = 120$ MeV is compatible with

experimental results obtained in [12, 13]. In this sense, this set of states represents a realistic simulation of a large number of inelastic couplings.

For energies above (but near) the barrier, the discrepancies observed in [10] between data and elastic scattering theoretical cross sections at backward angles can be removed considering the present set of couplings. We have also obtained a reasonable description of the data even at very high energies. The behavior of the theoretical cross sections, while the number of coupled states is increased, indicates that much better adjustments would be obtained if more states with higher excitation energies were explicitly considered in the coupled equations.

In the context of the optical model, many works have reported a significant energy dependence of the phenomenological OP that fits elastic scattering data. The OP is composed of the bare and polarization potentials, the latter containing the contribution arising from nonelastic couplings. The bare potential is related to the effective nucleon–nucleon interaction within the context of the folding models. It is already well known that the OP can present a strong energy dependence for energies around the Coulomb barrier [3]. This behavior, coined the threshold anomaly, is related to the closure of the reaction channels at this energy region. On the other hand, the OP also presents significant energy dependence when observed within the context of a much wider energy range, from near-barrier to intermediate bombarding energies. Several theoretical models have been proposed to account for this energy dependence. So far, most of these models relate the OP energy dependence to the bare interaction, through the effective nucleon–nucleon interaction (e.g. [4–7]). Since the bare interaction assumed in the present CC calculations is energy independent, our results represent a strong indication that significant part of this OP energy dependence can be related with couplings to a large number of states of high excitation energies. The development of more efficient methods to solve coupled equations with these characteristics would be very important to improve the study of elastic scattering at intermediate energies.

Acknowledgments

We thank Professor M N Harakeh for discussions about results obtained in [12, 13]. This work was partially supported by the Fundação de Amparo à Pesquisa do Estado de São Paulo (FAPESP—Brazil) and the Conselho Nacional de Desenvolvimento Científico e Tecnológico (CNPq—Brazil).

References

- [1] Hagino K and Takigawa N 2012 *Prog. Theor. Phys.* **128** 1061
- [2] Balantekin A B and Takigawa N 1998 *Rev. Mod. Phys.* **70** 77
- [3] Brandan M E and Satchler G R 1997 *Phys. Rep.* **285** 143
- [4] Kobos A M, Brown B A, Hodgson P E, Satchler G R and Budzanowski A 1982 *Nucl. Phys. A* **384** 65
- [5] Kobos A M, Brown B A, Lindsay R and Satchler G R 1984 *Nucl. Phys. A* **425** 205
- [6] Chamon L C, Carlson B V, Gasques L R, Pereira D, de Conti C, Alvarez M A G, Hussein M S, Cândido Ribeiro M A, Rossi E S Jr. and Silva C P 2002 *Phys. Rev. C* **66** 014610
- [7] Hussein M S, Rego R A and Bertulani C A 1991 *Phys. Rep.* **201** 279
- [8] Chamon L C, Gasques L R and Carlson B V 2011 *Phys. Rev. C* **84** 044607
- [9] Chamon L C, Gasques L R, Alves L F M, Guimarães V, Descouvemont P, deBoer R J and Wiescher M 2014 *J. Phys. G* **41** 035101
- [10] Chamon L C, Gasques L R, Nobre G A P, Rossi E S Jr., deBoer R J, Seymour C, Wiescher M and Kiss G G 2015 *J. Phys. G* **42** 055102

- [11] de Vries H, de Jager C W and de Vries C 1987 *At. Data Nuclear Data Tables* **36** 495
- [12] Harakeh M N, van Heyst B, Van Der B and Van Der Woude A 1979 *Nucl. Phys. A* **327** 373
- [13] Brandenburg S, Borghols W T A, Drentje A G, Ekström L P, Harakeh M N and van der Woude A 1987 *Nucl. Phys. A* **466** 29
- [14] von Egidy T and Bucurescu D 2005 *Phys. Rev. C* **72** 044311
- [15] Thompson I J 1988 *Comput. Phys. Rep* **7** 167
- [16] Barnett A R and Lilley J S 1974 *Phys. Rev. C* **9** 2010
- [17] Karcz A, Kluska I, Sanok Z, Szmider J, Szymakowski J, Wiktor S and Wolski R 1972 *Acta Phys. Pol. B* **3** 525
- [18] Tickle R and Gray W S 1975 *Nucl. Phys. A* **247** 187
- [19] Hauser G, Löhken R, Rebel H, Schatz G, Schweimer G W and Specht J 1969 *Nucl. Phys. A* **128** 81
- [20] Goldberg D A, Smith S M, Pugh H G, Roos P G and Wall N S 1973 *Phys. Rev. C* **9** 1938
- [21] Bonin B *et al* 1985 *Nucl. Phys. A* **445** 381
- [22] Yusa S, Hagino K and Rowley N 2012 *Phys. Rev. C* **85** 054601
- [23] Keeley N, Lilley J S and Christley J A 1996 *Nucl. Phys. A* **603** 97